1. Introduction

This work involves the study of the mixing characteristics in a slurry bubble column reactor for the dehydration of isobutanol to isobutylene. The experiments were conducted in the Alternate Fuels Development Unit (AFDU) at La Porte, Texas. Powdered alumina based dehydration catalyst (30~34 wt % loading) suspended in an inert hydrocarbon oil forms the batch slurry phase. Isobutanol is bubbled as vapor through a sparger mounted at the bottom of the reactor. Most of the isobutanol fed to the reactor is converted to isobutylene and other by-products, while the small amount of unconverted isobutanol is separated and sent to a tank.

The chemistry for the dehydration of isobutanol to isobutylene is:

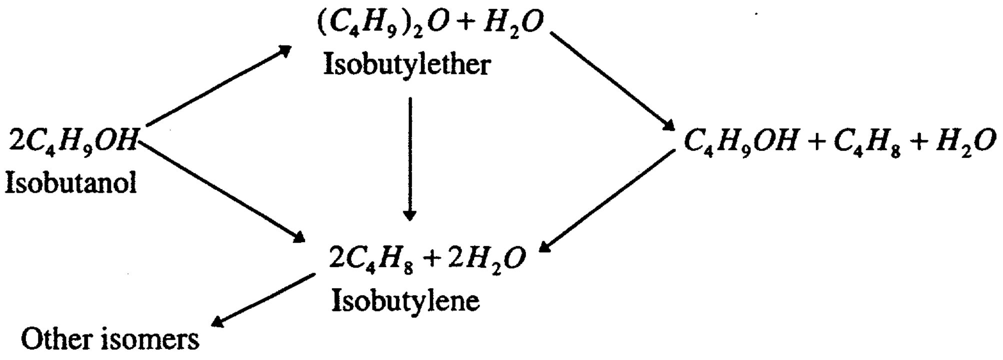

At the operating conditions used, the conversion of isobutanol was nearly complete and the total butene selectivity was equal to more than 98.0%. Based on the reaction stoichiometry shown above, the volume of the gas is doubled. Therefore the outlet superficial velocity of the gas is almost doubled as shown in Table 1, in which other experimental conditions are also listed.

2. Objectives

The objective of this work is to study the mixing characteristics of the gas and liquid phase in the slurry bubble column reactor by using radioactive tracer experiments. An examination of the tracer responses can provide some estimation of the back-mixing

Table 1. Tracer Experiments Conditions

Run No.	*Pressure, psig*	*Temp., °C*	*Injection, V=vapor L=liquid*	*Inlet Vel., cm/s*	*Outlet Vel., cm/s*	*Space Vel., SL/h•kg OXD**	*Vapor void, fraction, %*
R8.1-1	25.09	300.0	V	3.60	6.71	115	10-13
R8.1-2	25.09	300.0	V	3.60	6.71	230	10-13
R8.1-3	25.09	300.0	V	3.60	6.71	230	10-13
R8.2-1	24.94	299.7	V	7.01	13.72	230	13-15
R8.2-2	24.94	299.7	V	7.01	13.72	230	13-15
R8.3	24.94	299.7	L	7.01	13.72	230	13-15
R8.4	24.94	299.7	L	7.01	13.72	230	13-15
R8.5-1	24.84	300.4	V	9.75	18.90	315	14-16
R8.5-2	24.84	300.4	V	9.75	18.90	315	14-16
R8.6-1	25.22	299.8	V	12.19	24.08	400	16
R8.6-2	25.22	299.8	V	12.19	24.08	400	16
R8.7	25.22	299.8	L	12.19	24.08	400	16
R8.8	25.22	299.8	L	12.19	24.08	400	16

* OXD: Oxidants Catalyst

parameters which are essential in reactor design and simulations. Interpretation of the tracer data at this stage is based on the one dimensional axial dispersion model (ADM). The ADM is chosen because it is relatively simple and is one of the most frequently used models in reactor design and performance calculations. It was also chosen for completeness since methanol synthesis runs were also interpreted based on the ADM. We wanted to compare the results obtained in two different systems.

However, our long term goal is to assess the suitability of the present model (ADM) to describe mixing in the gas and liquid phase in slurry bubble column reactors and suggest alternatives, if necessary.

3. Gas Holdup Measurement

Gas holdup measurements in the reactor were conducted by using the Nuclear Density Gauge (NDG) method. The details of this technique were described in the report on tracer studies of the slurry bubble column for methanol synthesis (Degaleesan et al, 1996). Briefly, it is a noninvasive method in which a source emits a narrow beam of radiation through the slurry column. A detector which is located at 180° to the beam receives the radiation. The source - detector pair can be moved so as to scan the cross section of the column and provide a series of chordal measurements. Usually average gas holdup is obtained by this method, using the measurement only along a single chord, most often along the diameter. However, the gas holdup obtained is then higher than the actual cross sectional average value as discussed in the previous report. (Degaleesan et al, 1996). The gas holdup for various experimental conditions is shown in Appendix 1 as a function of position along the reactor. One can observe that the gas holdup increases linearly with axial position, responding to the increase of gas volumetric flow rate caused by reaction. Based on the data given in Appendix I, expressions for the linear variation of gas holdup with axial position z for different conditions, were obtained:

$$U_{gin}=3.66\text{ cm/s:}\quad \varepsilon_g = 1.77\times10^{-4}\,z + 0.080 \quad (\text{z in cm}) \tag{1}$$

$$U_{gin}=7.01\text{cm/s:}\quad \varepsilon_g = 2.16\times10^{-4}\,z + 0.125 \quad (\text{z in cm}) \tag{2}$$

$$U_{gin}=10.67\text{ cm/s:}\quad \varepsilon_g = 2.16\times10^{-4}\,z + 0.162 \quad (\text{z in cm}) \tag{3}$$

$$U_{gin}=12.19\text{cm/s:}\quad \varepsilon_g = 2.56\times10^{-4}\,z + 0.170 \quad (\text{z in cm}) \tag{4}$$

In the above expressions, U_{gin} is the inlet superficial gas velocity in (cm/s), ε_g is the gas holdup and z is the axial coordinate in cm.

4. Tracer Experiments

A schematic of the AFDU slurry bubble column reactor is shown in Figure 1. It has a height (from bottom to top) of 8.63 m and an inside diameter of 0.57 m. The maximum slurry level is about 6.10 m (L/D ratio of 10.7) with the remainder being vapor disengagement space. The reactor contains an internal heat exchanger consisting of ten 1 inch tubes. These tubes occupy less than 5% of the reactor cross section. A nuclear density gauge used to measure the gas holdup is mounted on an external track and spans the space occupied by the internal heat exchanger. Radioactive Ar-41, used to study the residence time distribution of the vapor phase, was injected as a pulse at the inlet of the reactor. Radioactive Manganese-56 (50 μm) particles mixed in oil were used for liquid (slurry) phase tracing. There were two injection ports, the top T-nozzle, 3.99 m from the bottom of the reactor, and the bottom T-nozzle, 2.57 m from the bottom of the reactor. The axial levels of the two injection ports are shown in Figure 1.

Radiation measurements for the vapor and liquid tracers were conducted by using a number of 2" by 2" NaI scintillation detectors positioned outside the column, at various axial levels as shown in Figure 1. Four sets of detectors were arranged along the column. For each set, there were four detectors placed at the same plane and at 90 degree angles with each other. In addition, detectors were placed at the inlet and outlet of the reactor. For liquid tracer injection, the inlet detector was placed just above the injection port to monitor the shape of the injected pulse.

The radiation measurements (intensity counts) obtained from the detectors at each axial position are used to generate normalized impulse response of the radioactive tracer at that position. For the purpose of analysis of the tracer data with the one dimensional axial dispersion model (ADM), for both the vapor and liquid phase, the responses from the four detectors at each level are averaged to obtain a cross sectional averaged response at the corresponding level. This is done because the one dimensional axial dispersion model does not have the capability of resolving radial and azimuthal variations.

The total radiation (intensity count) recorded at the detector is an integral of the contribution of the entire mass (or volume) of the tracer, which can be considered to

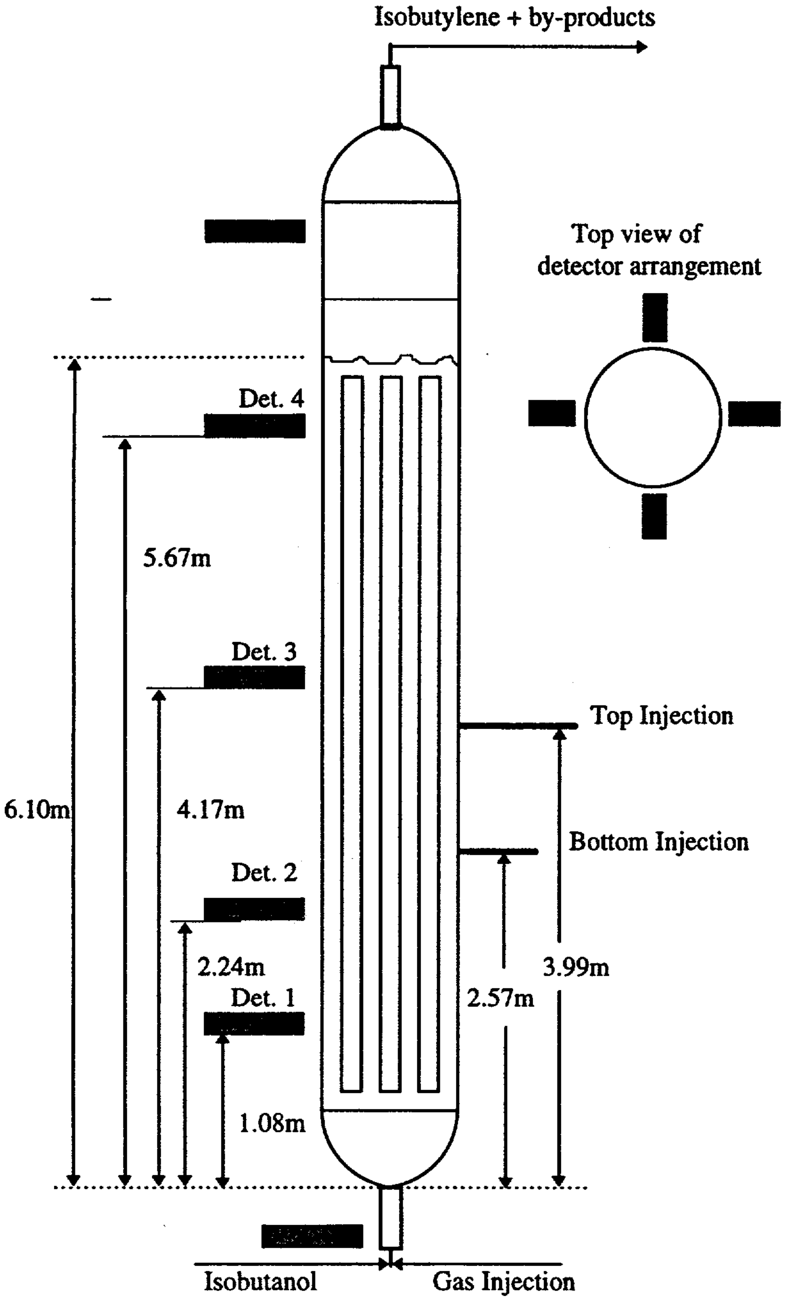

Figure 1. Schematic of the Reactor for Tracer Experiments

comprise of individual point sources within the field of view of the detector. For the tracer experiments considered in this study, the detectors were shielded on their sides. Therefore, only the front circular surface of the detectors could see the radiation. By using this configuration, the spatial range from which a detector receives most of its signal is assessed. The equations used for this calculation (Tsoulfanidis , 1983) are shown in Appendix II of the Methanol report (Degaleesan et al , 1996). For a uniform distribution of radioactive tracer in the column, it can be shown that more than 90 percent of the intensity recorded at a detector, shielded on its sides, comes from a small volume (less than 1 percent of the entire reactor volume) which is the closet to the face of the detector. This is illustrated in Figure A. 2.1 of the methanol report (Degaleesan et al, 1996), where the exponential decay in radiation intensity with distance can be seen.

For gases and liquids, which are no longer point sources, the specific activity, defined as the number of disintegrations/time/volume of the nuclei of the radioisotope, depends on the mass or volume of the radioactive source (Tsoulfanidis, 1983), and thereby on the local concentration of tracer.

Since the one dimensional ADM, when applied to the liquid and gas phase, can only consider uniform tracer concentration and phase holdup distribution in any given cross section, the intensity recorded at the detector is assumed to be directly proportional to the concentration of tracer at a given axial location of the column . The liquid Mn-56 tracer, with a half life of 2.58 hr, emits γ radiation at 0.85 MeV. Since this tracer remains confined only to the liquid (slurry) phase, the average detector response is directly proportional to the tracer concentration in the liquid phase. However, the gas tracer Ar-41 with a half life of 1.29 hr, emitting γ rays at 1.29 MeV, is soluble in the liquid. Therefore, for the gas tracer experiments, the total tracer concentration, at a given time and axial position, which is assumed to be proportional to the average detector response, is taken to be

$$C_t(t,z) = \varepsilon_l C_l(t,z) + \varepsilon_g C_g(t,z) \qquad (5)$$

5. Modeling

In the present study, the one dimensional axial dispersion model (ADM) is used to model the flow pattern and mixing of the liquid and gas phase. Basically, it is a plug flow model with axial dispersion superimposed on it.

5.1 Liquid Phase Tracer

For batch operation of the liquid (slurry) phase with a non-volatile liquid tracer, the one dimensional axial dispersion model can be written as:

$$\frac{\partial C_l}{\partial t} = D_l \frac{\partial^2 C_l}{\partial z^2} \tag{6}$$

Initial and boundary conditions are:

$$t = 0, \qquad C_l = \delta(t)\delta(z - z_i) \tag{7}$$

$$z = 0, \quad z = L, \qquad \partial C_l / \partial z = 0 \tag{8}$$

Here z_i and L are the tracer injection level and the given detector level, respectively. An analytical solution can be obtained with the axial dispersion coefficient D_l as the only parameter:

$$C_l(t, z) = 1 + 2\sum_{n=1}^{\infty} \cos(\frac{n\pi}{L} z_i) \cos(\frac{n\pi}{L} z) \exp(-D_l n^2 \pi^2 t) \tag{9}$$

The residence time distribution (RTD) theory (Nauman, 1987; Dudukovic, 1987) suggests that parameters in a model can be found by minimizing the sum of the square of errors between model predictions and experimental data. Thus, the objective function is chosen as :

$$F = \min \sum_{i=1}^{N_p} (\frac{R(t_i, z)}{R_{\max}} - \frac{C_l(t_i, z)}{C_{l\max}})^2 \tag{10}$$

where $R(t_i, z)$ is the averaged intensity of the four detectors at the same level and $R_{\max}$ is the maximum value of intensity at z, $C_l(t_i, z)$ is the predicted tracer concentration by the model, and $C_{l\max}$ the maximum value of predicted tracer concentration by the model. N_p is the number of data points, 4000 in this study.

Time domain fitting of the model prediction with the averaged detector response at every level is performed for each injection, to estimate the model parameter D_l. It should be pointed out that the tracer injection here is a point injection but not a perfect uniform cross sectional injection which Equation (7) requires. A finite time is needed for the tracer to spread radially and form a uniform distribution in the radial direction.

5.2. Gas Phase Tracer

Since the gas phase tracer Ar-41 is soluble in the liquid phase, the one dimensional axial dispersion model with interfacial mass transfer is necessary for modeling the Argon tracer distribution in the reactor. The mass balance equations for the tracer in the gas and liquid phase can be written as follows:

$$\frac{\partial C_g}{\partial t} = D_g \frac{\partial^2 C_g}{\partial z^2} - \frac{U_g}{\varepsilon_g}\frac{\partial C_g}{\partial z} + k_l a (C_l - C_g / H) \qquad (11)$$

$$\frac{\partial C_l}{\partial t} = D_l \frac{\partial^2 C_l}{\partial z^2} - \frac{\varepsilon_g}{\varepsilon_l} k_l a (C_l - C_g / H) \qquad (12)$$

The initial and boundary conditions are:

$$t = 0, \quad C_l = 0, \quad C_g = 0 \qquad (13)$$

$$z = 0, \quad \partial C_l / \partial z = 0, \quad U_g C_g / \varepsilon_g = D_g \partial C_g / \partial z + U_g \delta_i(t) / \varepsilon_g \qquad (14)$$

$$z = L, \quad \partial C_l / \partial z = 0, \quad \partial C_g / \partial z = 0 \qquad (15)$$

where, D_g and D_l are the gas and liquid phase axial dispersion coefficients, H is the Henry's law constant defined as $(C_g / C_l)_{eq}$, $k_l a$ is the volumetric liquid film mass transfer coefficient, U_g is the gas superficial velocity, ε_g and ε_l are the gas and liquid (slurry) phase holdups, respectively. The function $\delta_i(t)$ describes the pulse of tracer injected. For a perfect impulse injection, $\delta_i(t) = \delta(t)$ where $\delta(t)$ is the Dirac delta function. Other symbols are explained in the Nomenclature.

From two phase mass transfer theory we know that the overall mass transfer coefficient and the film mass transfer coefficients are related by the following equation:

$$\frac{1}{K_l a} = \frac{1}{k_l a} + \frac{1}{H' k_g a} \qquad (16)$$

where $K_l a$ is the overall volumetric mass transfer coefficients, $k_l a$ is the liquid film volumetric mass transfer coefficient, $k_g a$ is gas film volumetric mass transfer coefficient, $H^{'}$ is the customary Henry's law constant defined as

$$H^{'} = (\frac{p_g}{C_l})_{eq} \tag{17}$$

For slightly soluble gases in liquid, like Ar-41 in hydrocarbon oil, $H^{'} k_g a >> k_l a$, so $K_l a \cong k_l a$.

Impulse response measurements were performed for the gas phase tracer injected into the vapor phase at the reactor inlet. The tracer was injected as a pulse into the inlet gas line upstream from the gas distributor. A detector was placed just above the injection point to monitor the input pulse. Thus, the responses detected by this detector are used to simulate the input pulse to the reactor for the purpose of modeling. In the present study, the gas tracer input function $\delta_i(t)$ is not a perfect impulse , instead of using delta function, we use the following Gaussian function to match the response of the inlet detector to the input function $\delta_i(t)$:

$$\delta_i(t) = \frac{N_c}{\sqrt{2\pi D_i t}} \exp[-\frac{(l_i - U_g t)^2}{2 D_i t}] \tag{18}$$

D_i , l_i and N_c are the parameters used to match the simulated pulse with the measured responses of the inlet detector. It has been found that this model provides very good fits to the inlet detector responses. An example of the inlet pulse fitting is shown in Figure 2, while others can be found in Appendix II. Table 2 shows the parameters of the input pulse which were estimated for different runs. It was found that the parameters obtained by fitting model predictions to gas phase tracer data were very sensitive to the shape of the inlet pulse. Hence, good representation of the inlet pulse rather than using an assumed delta function was deemed necessary.

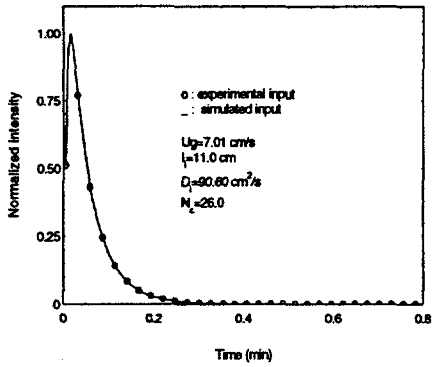

Run No. : R82-2

Figure 2. Input pulse fitting

Table 2. Simulation results of the input pulse

	N_c	D_i , cm²/s	l_i , cm
R82-1	28.0	98.96	11.5
R82-2	26.0	90.60	11.0
R86-1	65.0	433.3	25.5
R86-2	66.0	493.3	25.0

6. Parameter Estimation

6.1 Liquid Tracer

Four liquid tracer injections were made at two different positions. It was observed that in most cases the detector responses close to the injection point exhibit overshoots, even some responses far from the injection point show overshoots to some extent. At present, parameter estimation is conducted only for those responses which do not exhibit overshoots. The results of fitting the model to data for all such cases are listed in Table 3. Typical fits to the experimental data are shown in Figure 3, while other results are listed in Appendix III.

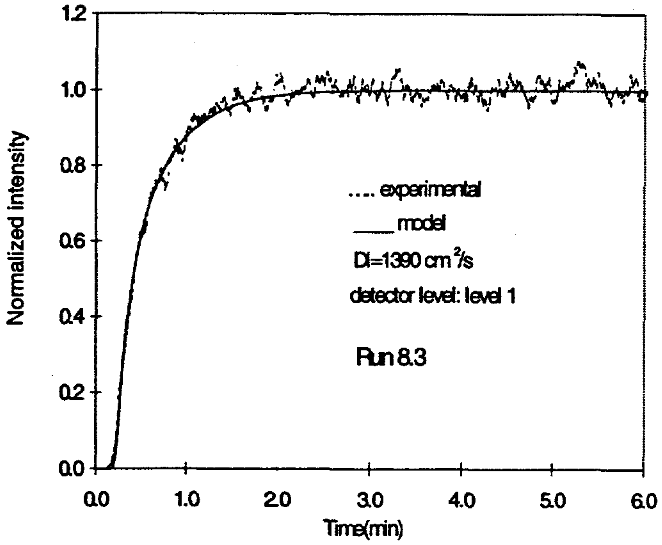

Run No. : R83

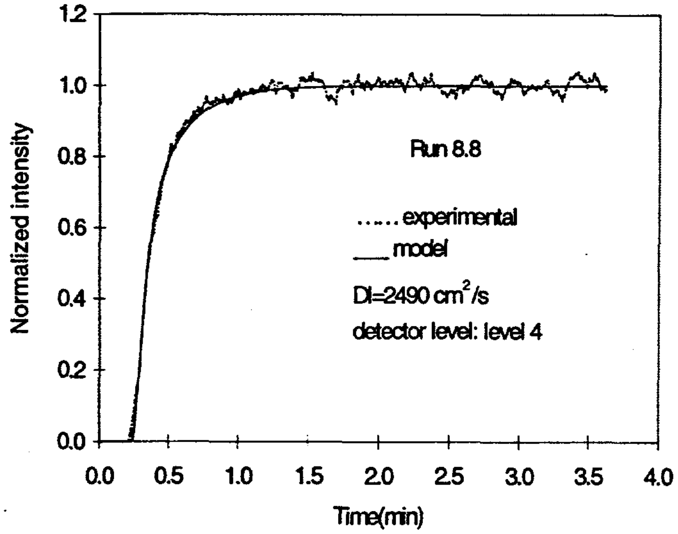

Run No. : R88

Figure 3. Model fits of experimental responses for the liquid tracer

Table 3 Estimated Axial Dispersion Coefficient for the Liquid Tracer

Run No.	U_g, cm/s	Gas holdup, $\bar{\varepsilon}_g$	Injection	Detector level	D_l, cm^2/s
R8.3	7.01	0.19	1	1	1390
				3	*
				4	*
R8.4	7.01	0.19	2	1	*
				2	*
				3	5390
				4	2990
R8.7	12.89	0.25	1	1	2350
				2	*
				3	*
				4	*
R8.8	12.89	0.25	2	1	*
				2	*
				3	6000
				4	2490

*: The response exhibits a strong overshoot

6.1.1 Discussion

From the plots of experimental responses and model predictions and the D_l values shown in Table 3, some observations can be made:

1) Injection levels

Two injection levels were used in the liquid tracer study, 3.99 m (1) and 2.57 m (2) above the bottom of the column, respectively. The averaged D_l values for the two different injection levels at the same gas velocity are different. This indicates that the distribution of the tracer in the axial direction of the column is non-symmetric, which is contrary to the nature of symmetric distribution for batch liquid operation in the one dimensional axial dispersion model.

2) Detector levels:

For the same injection, responses were detected at four different levels. The values of D_l at different detector levels for the same injection are very different. The reason for this is the non-uniform distribution of liquid tracer injection at a given axial location, which cannot be accounted for by the one dimensional ADM. For the present experiments, the injection at a given level is away from the wall (about 2 inches), into the region of liquid upflow. Therefore the fitted dispersion coefficients D_l for the responses of the detectors at level 3, which is above the lower injection level are much higher than those obtained at other levels, since most of the tracer injected at the lower level is predominantly carried upward by convection in this region.

4) Gas velocity

At a given velocity, D_l is averaged for all the injections and levels but only for the experimental responses with no overshoots. The averaged D_l are 3260 cm^2/s and 3610 cm^2/s at gas superficial velocities of 7.01 cm/s and 12.19 cm/s, respectively. A small increase in the axial dispersion coefficient with gas velocity was observed. Since only a small number of data points is available, this is not sufficient to conduct any statistical analysis of this result.

From the averaged values of the axial dispersion coefficient we can conclude that a reasonable degree of liquid (slurry) mixing in the column exists at the present operating conditions. The characteristic liquid mixing time based on the entire dispersion height is in the range of L^2/D_l : 109~121 seconds. The effect of this extent of mixing on reactor performance depends on the characteristic reaction time.

The liquid dispersion coefficients obtained in this study are compared with correlations from the literature (Kato et al, 1972; Baird and Rice, 1975; Deckwer et al., 1974). The correlations applicable to the column diameter and operating conditions used are listed in Table 4 as well as the predicted liquid axial dispersion coefficients. The predicted values of D_l are always smaller than those obtained by parameter fitting of the experimental responses.

There are several reasons for this. One of the reasons is due to the non-uniform injection of tracer into the column. Since the tracer is injected into the region where the liquid flow is predominantly upward due to convection, the tracer arrives faster at the detector levels above the points of injection, and this results in higher values of the axial dispersion coefficient, which is used to model all the effects leading to liquid mixing in the column. In addition to this, the experiments are performed in a high pressure system (around 2 atm) which will increase liquid backmixing in the column when compared with literature correlations which are valid at atmospheric pressure. Another important factor is the effect of the expanding gas in the system which results in higher gas flow rates up the column and therefore more convection and turbulence in the system, which would result in larger D_l.

6.1.2 Conclusions and Future Work

The axial dispersion model (ADM) has been fitted to tracer responses without overshoots, in line with what was done for the methanol runs, and reasonably good fits are obtained. However, the values of the estimated D_l are very scattered at different axial locations for the same injection, as well as for different injection levels at the same detector level. The averaged axial dispersion coefficients show a small increase with the increase in superficial gas velocity. The magnitude of the estimated D_l indicates that a reasonable extent of back mixing exists for the liquid phase (slurry phase). The responses with overshoots and possible match by the ADM will be discussed in a separate report.

To match better the data at all detector levels, a phenomenological model that captures the essence of the fluid dynamic behavior of the system should be used. The Recycle with Cross Flow and Dispersion Model (RCFDM), proposed recently by the CREL group (Degaleesan et al, 1996), seems a good alternative in the description of liquid mixing. A preliminary analysis of the model has been done, indicating a good agreement between experimental responses and model simulation. This will be described in the follow up report.

Table 4. Liquid Dispersion Coefficient Predicted by Various Correlations

Investigator	Equation (in SI)	Range of Variables	Predicted D_l, cm^2/s
Kato and Nishiwaki (gas-liquid-solid)	$D_l = \dfrac{U_g D_c}{\dfrac{13Fr^{0.5}}{1+8Fr^{0.425}}}$ $Fr = U_g^{\ 2} / gD_c$	$0.066 \le D_c \le 0.21$ m $0.003 \le U_g \le 0.30$ m/s	1620 ($U_{g,in}$=7.01cm/s) 1970 ($U_{g,in}$=12.19cm/s)
Baird and Rice (gas-liquid)	$D_l = 0.35 D_c^{4/3} (gU_g)^{1/3}$	$0.082 \le D_c \le 1.53$ m $0.003 \le U_g \le 0.45$ m/s	1610 ($U_{g,in}$=7.01cm/s) 2000 ($U_{g,in}$=12.19cm/s)
Deckwer et al (gas - liquid)	$D_l = 0.678 D_c^{1.4} U_g^{\ 0.3}$	-	1560 ($U_{g,in}$=7.01cm/s) 1850 ($U_{g,in}$=12.19cm/s)

6.2 Gas Tracer

Gas tracer experiments were conducted at four different inlet superficial gas velocities, namely 3.60 cm/s, 7.01cm/s, 9.75 cm/s and 12.19 cm/s. However, only two of these, 7.01 cm/s and 12.19 cm/, have the corresponding liquid tracer runs at the same inlet gas superficial velocities. Therefore, parameter estimation was conducted only for these two runs. As mentioned before, the gas tracer Ar-41 is soluble in the liquid phase, so that mass transfer occurs between the liquid phase and gas phase. The partial differential equations, Eq (11) to Eq. (15), are solved numerically. For the gas phase model, seven parameters, D_l, D_g, H, k_la, U_g, ε_g, ε_l, need to be evaluated. However, not all of the parameters need to be estimated by response fitting. D_l can be obtained from the liquid phase results at the same gas inlet superficial velocities, ε_g is available from experimental measurements (provided by Air Products and Chemicals) and $\varepsilon_l = 1 - \varepsilon_g$ (pseudo-homogeneous phase is assumed for liquid and solid phase), U_g is known from the gas inlet and outlet superficial velocities (provided by Air Products and Chemicals) and based on an assumption of the type of variation of U_g with axial direction. Parameter fitting is again performed by minimizing the sum of the square of errors with Equation (10). The five cases considered here are listed in Table 5. In case 1, three floating parameters D_g, H, k_la, are fitted so that the results can be compared with the methods involving only two-floating parameters in which the Henry's law constant H is treated as a known constant calculated from thermodynamics (case 2).

6.2.1 Case 1: Three Floating Parameters D_g, H, k_la

In this case, ε_g and U_g are used as inputs to the model. The mean ε_g and U_g calculated from their inlet and outlet values are used in fitting of the tracer data. Results for the model parameters obtained by fitting the model to the various experimental responses at different detector levels are tabulated in Table 6. Figure 4 shows the typical fits of the model to experimental responses. Table 6 also lists the start time for each run obtained from model fitting.

- **Discussion**

Henry's law constant H is estimated by fitting the experimental responses with the model as well as the gas axial dispersion coefficient D_g and liquid film volumetric mass transfer coefficient k_la. We can now compare the value of H estimated from curve fitting with the values obtained from thermodynamic calculations. At the present operating conditions, the Henry's law constant H is 106 from thermodynamic calculations (Bhatt, 1995). It is obvious that H estimated by parameter fitting is much smaller as shown in Table 6. The average values of H, at gas velocities of 7.01 cm/s and 12.19 cm/s, are 5.8 and 6.1 respectively, which are much smaller than 106.0. Meanwhile, the corresponding average gas axial dispersion coefficients D_g are 2960 cm^2/s and 4890 cm^2/s, respectively, which are also smaller than those obtained by parameter fitting of the tracer data with H as a fixed input parameter (106.0 in this study) as shown in the subsequent cases 2-6. This indicates that with the three floating parameters, the Henry's law constant H would be underestimated as well as the axial dispersion coefficient D_g. In the earlier paper (Toseland, et al, 1995), the same parameter estimation was performed for one of the two runs at inlet superficial gas velocity of 7.01 cm/s. However, the third term and the second term of the left hand sides of Eq. (1) and Eq. (2) in their paper was $k_la(HC_l-C_g)$ instead of $k_la(C_l-C_g/H)$ in the present model, Eq. (11) and Eq.(12). If we denote the equilibrium constant used in Toseland et al.(1995 as H_T and their volumetric mass transfer coefficient as $(k_la)_T$ then the relation of their parameters and those used in the present report are $(k_la)_T H_T = k_la$ and $H_T = H$. In addition, in the present study an input function that exactly matches the gas phase tracer input impulse has been used, which is different from the one used by Toseland et al. (1995). Therefore an exact comparison between the model parameters obtained in this study and those of Toseland et al. (1995) cannot be made. The variation arising in the model parameters due to the different input functions used is shown in Table7, which compares the model parameters obtained in this study and the results from Toseland et al. (1995).

Table 5. Different Cases Used to Match the Model with Experimental Responses.

Case No.	Fixed Parameters (input parameters)	Floating parameters
1	$U_g = \overline{U}_g$, $\varepsilon_g = \bar{\varepsilon}_g$, $D_l = D_l$(liquid)	D_g, H, $k_l a$
2	$U_g = U_{g,in}$, $\varepsilon_g = \bar{\varepsilon}_g$, $D_l = D_l$(liquid), $H = H$(thermo.)	$D_g, k_l a$
3	$U_g = \overline{U}_g$, $\varepsilon_g = \bar{\varepsilon}_g$, $D_l = D_l$(liquid), $H = H$(thermo.)	$D_g, k_l a$
4	$U_g^{\,i} = \overline{U}_g^{\,i}$, $\varepsilon_g^{\,i} = \bar{\varepsilon}_g^{\,i}$ $D_l = D_l$(liquid), $H = H$(thermo.)	$D_g, k_l a$
5	$U_g = U_{g,in} + (U_{g,f} - U_{g,in}) z / l_{\min}$ $\varepsilon_g = c + d\varepsilon_{g,in}$ $D_l = D_l$(liquid), $H = H$(thermo.)	$D_g, k_l a$, $l_{\min}$
6	$U_g = U_{g,f} + (U_{g,in} - U_{g,f})(1 - z/Z) e^{-\beta z}$ $\varepsilon_g = c + d\varepsilon_{g,in}$ $D_l = D_l$(liquid), $H = H$(thermo.)	$D_g, k_l a$, β

Table 6. Case1 : Parameter Estimation Results for Gas Tracer Experiments

Run No.	$\bar{U}_g$, cm/s	$\bar{\varepsilon}_g$	D_l, cm^2/s	Detector Level :	Start time, min	Model Parameters D_g, cm^2/s	H	$k_l a$ s^{-1}
R82-1	10.37	0.19	3260	1	0.25	1130	2.25	14.98
				2		3130	4.14	4.57
				3		2320	6.92	0.90
				4		3760	6.69	0.60
R82-2	10.37	0.19	3260	1	0.38	1630	3.12	17.98
				2		1680	4.81	7.82
				3		5420	12.38	0.64
				4		4610	6.14	0.18
R86-1	18.14	0.25	3610	1	0.25	1860	3.11	4.22
				2		6830	7.14	3.03
				3		8260	7.37	0.031
				4		8040	6.89	0.078
R86-2	18.14	0.25	3610	1	0.22	1420	2.70	3.61
				2		3790	6.48	4.12
				3		2770	7.09	0.18
				4		6120	7.84	0.072

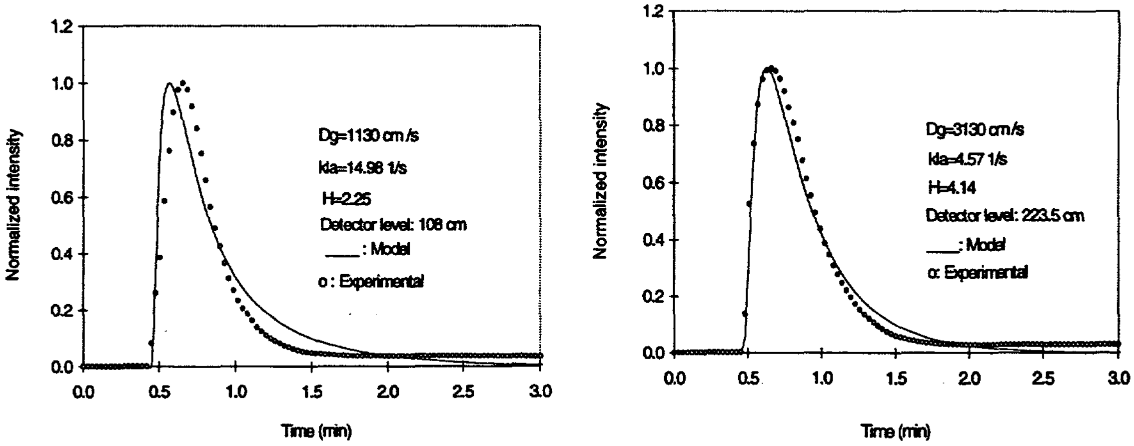

Run No. : R82-1

Run No. : R82-1

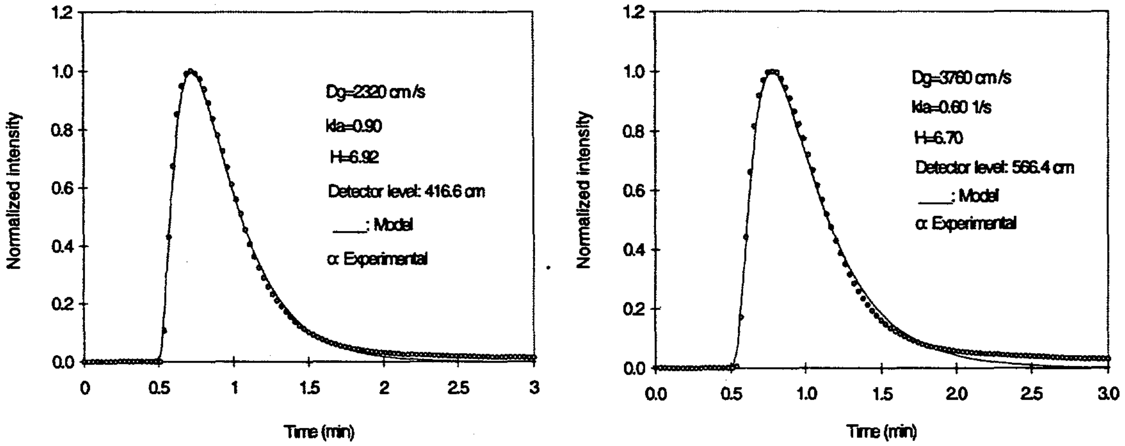

Run No. : R82-1

Run No. : R82-1

Figure 4. Case 1: Model Fits of Experimental Responses

Table 7. Comparison of the Average Estimated Parameters at $U_{g,in}$ =7.01 cm/s

	D_g, cm^2s	H	$k_l a$, s^{-1}
Present study	2960	5.81	5.96
Toseland et al(1995)	5810	5.43	0.24

and a different function was used to simulate the input impulses. The averaged D_g, H, $k_l a$ are 5810 cm^2/s, 5.43 and 0.24 s^{-1} respectively as shown in Table 7.

It is noted that the values of D_g at detector level 2 and detector level 3 are very different for Run86-1 and Run86-2, which were also performed at the same conditions. A calculation is conducted with ADM to investigate the effects of D_g on the response curves. In the calculation, the value of D_g at level 2 and level 3 of Run86-2 (3790 and 2770 cm^2/s) are replaced by those at level 2 and level 3 of Run86-1 (6830 and 8260 cm^2/s) while the values of H and $k_l a$ remain the same. Model predictions based on new D_g values are plotted in Figure 5 together with the model predictions based on the original D_g values (3790 and 2770 cm^2/s). It is clear that the model prediction do not vary much with different values of D_g. This means that in the present situation, the ADM is not very sensitive to the gas phase axial dispersion coefficients.

Model predictions have different sensitivities to the three parameters, D_g, H, $k_l a$. The model is the most sensitive to variations in H and the lest sensitive to $k_l a$ change. That is why the values of the estimated $k_l a$ are so much scattered (0.0312 s^{-1}~ 17.98 s^{-1}). The same situation was encountered in the tracer data parameter fitting for methanol synthesis, and was confirmed by a parameter sensitivity analysis (Degaleesan et al, 1996). This indicates that the axial dispersion model is not suitable for the estimation of mass transfer coefficient $k_l a$.

It is also noted that the experimental response curves at some detector levels for Run86-1 and Run86-2 have a long tail which does not come down to zero. These levels

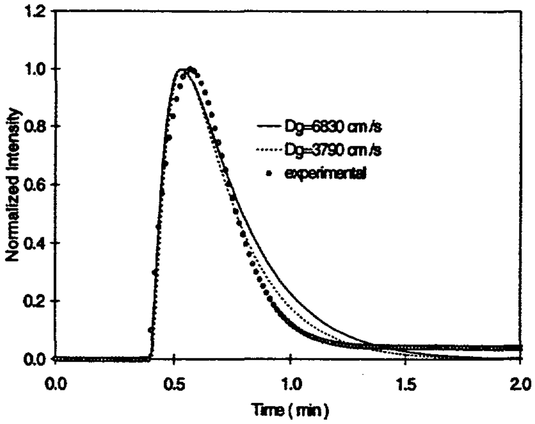

Run No. : R86-2, level 2

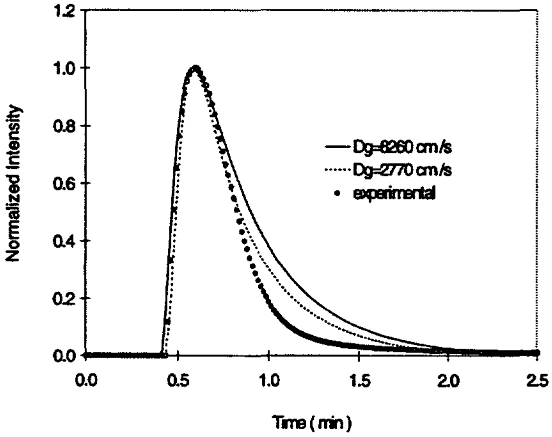

Run No. : R86-2, level 3

Figure 5. Comparison of model predictions with different D_g values

are: level 1, level 2 for Run86-1 and level 1, level 2 for Run86-2. The reason for the prolonged tails is not clear. However, these do affect model fitting.

6.2.2 Case 2: Two Floating Parameters D_g, $k_l a$ ($U_{g,in}$ and $\bar{\varepsilon}_g$ as inputs)

In this case, two floating parameters, D_g, $k_l a$, are estimated. The Henry's law constant H is now taken as a constant estimated from thermodynamics, 106.0 at the present operating conditions. The gas superficial velocity, U_g is taken as the inlet gas superficial velocity $U_{g,in}$ for the whole column and the gas holdup is taken as the averaged value along the column, 0.19 and 0.25 for the inlet gas superficial velocities of 7.01 cm/s and 12.19 cm/s, respectively. The estimated parameter values are shown in Table 8. Typical fits of model predictions with experimental responses are shown in Figure 6.

Some observations could be made from Table 8. First, the estimated gas axial dispersion coefficient values, D_g, are much larger than those obtained in Case 1, showing that if the Henry's law constant H is estimated from tracer curve fitting, the D_g thus obtained would be much smaller. Second, the values of the mass transfer coefficient, $k_l a$, shown in Table 8 are not so scattered as those in Case 1, ranging from 0.66 to 2.79 s^{-1}, which is in the usual range obtained by most investigators. The averaged axial dispersion coefficients are 5800 cm^2/s and 6320 cm^2/s for the inlet gas velocities of 7.01 cm/s and 12.39 cm/s, respectively. In this case the estimated $k_l a$ are less spread out ($k_l a_{\max} / k_l a_{\min} < 4.5$) than those obtained in other cases.

Generally, model fits for Run82-1 and Run82-2 are reasonably good, while model fits for Run86-1 and Run86-2 are somewhat off. Larger deviations between model predictions and experimental responses are observed at level 1 and level 2 of Run86-1 and Run86-2, where there is a long tail in the experimental response.

Since the gas volume increases from the bottom to the top of the reactor, the model in this case does not represent the actual conditions. However, from the results obtained in this case we learn the consequences of not accounting for the variation in gas volumetric flow rate in the reactor. Compared with the results obtained in the other cases that follow, and that account for gas flow rate variation, the axial diffusion coefficient D_g obtained in this case are smaller. Hence, it is necessary to incorporate the variation of gas velocity.

Table 8. Case 2: Parameter Estimation Results of Gas Tracer Experiments

Run No.	$U_{g,in}$ cm/s	$\bar{\varepsilon}_g$	D_l, cm^2/s	Detector Level :	Model Parameters	
					D_g, cm^2/s	$k_l a$ s^{-1}
R82-1	7.01	0.19	3260	1	6460	1.06
				2	4030	1.62
				3	6110	2.45
				4	4430	1.33
R82-2	7.01	0.19	3260	1	6430	1.52
				2	5470	2.11
				3	7370	1.25
				4	5510	1.30
R86-1	12.19	0.25	3610	1	4580	1.18
				2	7800	1.06
				3	6900	1.07
				4	5840	0.75
R86-2	12.19	0.25	3610	1	8360	1.25
				2	4830	1.34
				3	6370	2.79
				4	5890	0.66

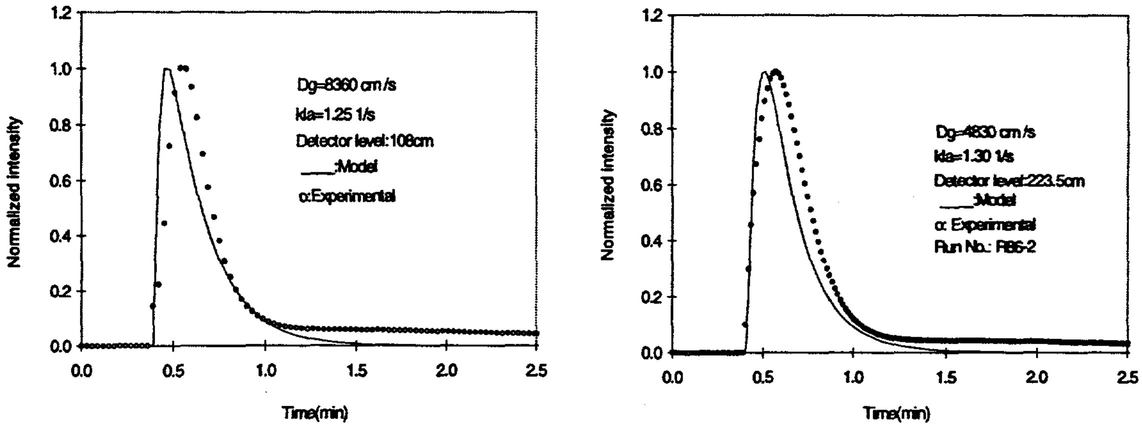

Run No. : R86-2

Run No. : R86-2

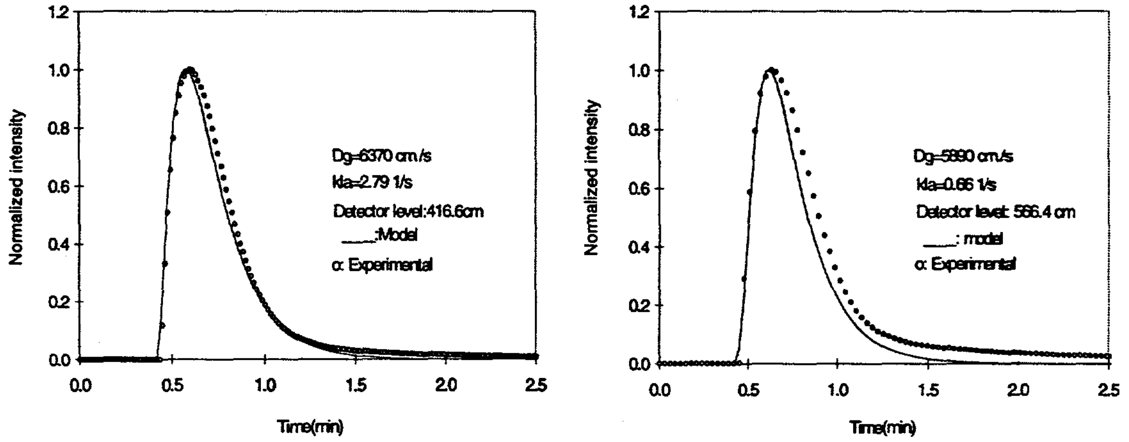

Run No. : R86-2

Run No. : R86-2

Figure6. Case 2: Model Fits of Experimental Responses

6.2.3 Case 3 : Two Floating Parameters D_g, $k_l a$ ($\overline{U}_g$ and $\bar{\varepsilon}_g$ as inputs)

In this case, we use the column averaged superficial gas velocity $\overline{U}_g$, instead of inlet superficial gas velocity as done in Case 2. The volumetric flow rate of the gas increases due to reaction, therefore the superficial gas velocity increases along the column from the bottom to the top. The averaged superficial gas velocity is obtained by averaging the inlet and outlet superficial gas velocities which are tabulated in Table 1. Parameter estimation was conducted to compare the results with those obtained in Case 1. The results are listed in Table 9 and the plots of model fits to experimental responses are shown in Figure 7. The averaged axial dispersion coefficients, at inlet superficial gas velocities of 7.01 cm/s and 12.19 cm/s, are 7190m^2/s and 8630 cm^2/s, respectively, showing a definite increase with the increase in gas velocity. It is also seen that the values of D_g obtained are higher than those in Case 2, indicating a larger extent of backmixing of the gas phase in the reactor. However, compared with Case 2, the estimated $k_l a$ values are more scattered, ranging from 0.12 to 12.27 (s^{-1})($k_l a_{\max} / k_l a_{\min} = 100$). As already mentioned, the parameter estimation via tracer fitting is the lest sensitive to $k_l a$, therefore, small changes in input parameters (gas holdup, superficial gas velocity) may cause large variations in $k_l a$.

In this case, the model fits for Run82-1 and Run82-2 seem reasonable, as can be seen from the plots. However, for Run86-1 and Run86-2, the model predictions and the experimental responses are way off. Run86-1 and Run86-2 were conducted at higher gas velocities than Run82-1 and Run82-2. Theoretically, the axial dispersion model predicts more backmixing at higher gas velocities. The reason for poor agreement of the model and data may be caused by the use of the overall mean $\overline{U}_g$ and $\bar{\varepsilon}_g$ in the model fitting procedure. In addition, the L/D in this study may not be large enough to allow a one dimensional flow pattern to develop.

Table 9. Case 3: Parameter Estimation Results for Gas Tracer Experiments

Run No.	$\bar{U}_g$, cm/s	$\bar{\varepsilon}_g$	D_l, cm^2/s	Detector Level :	Model Parameters	
					D_g, cm^2/s	$k_l a$ s^{-1}
R82-1	10.37	0.19	3260	1	6650	1.20
				2	5340	1.14
				3	6480	1.54
				4	6410	1.04
R82-2	10.37	0.19	3260	1	8810	0.12
				2	8280	5.81
				3	8180	2.33
				4	7350	1.10
R86-1	18.14	0.25	3610	1	8900	12.27
				2	9240	0.76
				3	6780	0.90
				4	8580	0.71
R86-2	18.14	0.25	3610	1	8940	0.80
				2	9880	0.81
				3	8530	1.14
				4	8200	0.81

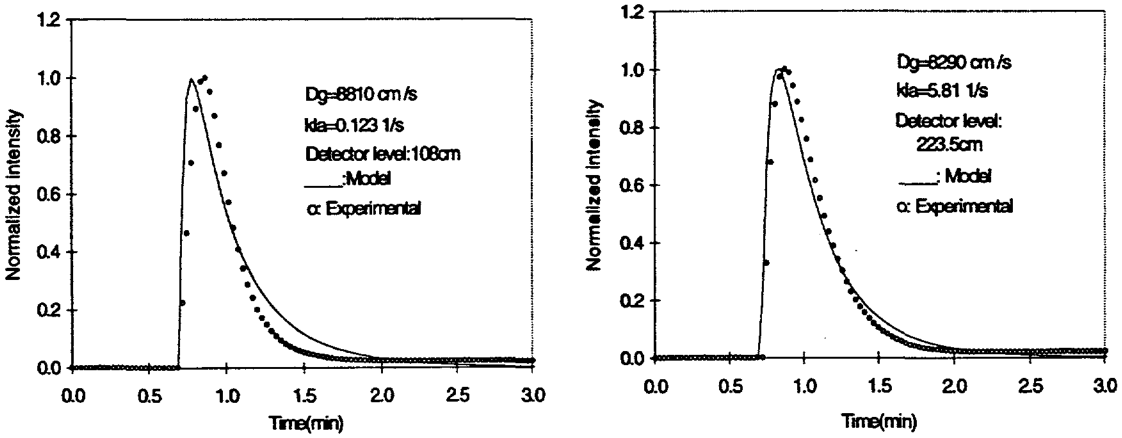

Run No. : R82-2

Run No. : R82-2

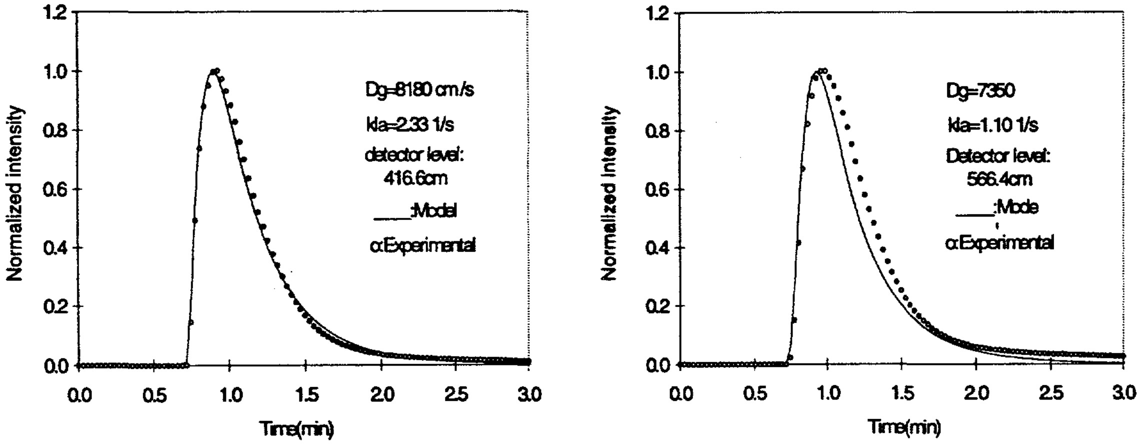

Run No. : R82-2

Run No. : R82-2

Figure 7. Case 3. Model Fits of Experimental Responses

6.2.4 Case 4: Two Floating Parameters, $D_g, k_l a$ ($\overline{U}_g{}^i$ and $\bar{\varepsilon}_g{}^i$ as inputs)

Since the gas holdup and gas superficial velocity vary in the axial direction of the reactor and the detectors are mounted at different axial positions along the column, it should be more reasonable to use different average gas holdup and superficial velocity for the responses obtained by detectors at different levels. In this case, the gas holdup and superficial gas velocity are averaged from the bottom of the reactor to the axial position at which the experimental responses, which are used for the parameter estimation, are acquired by the four detectors. For different levels, the average $\bar{\varepsilon}_g$ and $\overline{U}_g$ used in fitting are shown in Table 10.

Table 10. The average $\bar{\varepsilon}_g$ and $\overline{U}_g$ for different levels

		Level 1	Level 2	Level 3	Level 4
$\bar{\varepsilon}_g$	R82-1 R82-2	0.14	0.15	0.17	0.19
	R86-1 R86-2	0.18	0.20	0.22	0.24
$\overline{U}_g$	R82-1 R82-2	7.59	8.21	9.24	10.34
	R86-1 R86-2	13.20	14.28	16.06	17.98

The parameter estimation results are shown in Table 11 and the plots of model fits of and the experimental responses are shown in Figure 8. It is seen from Table 11 that for some detector levels, very small values of mass transfer parameter, $k_l a$, were obtained, for example, the values at level 1 and level 2 of Run82-1, level 1, level 2, level 3 of Run82-2. The ratio of $k_l a_{\max} / k_l a_{\min}$ is about 840! It is also observed that the very small (or very large) values of $k_l a$ always occur at the first and second levels of the detectors for almost all the cases considered in this study. This may also be attributed to the poor

Table 11. Case 4: Parameter Estimation Results of Gas Tracer Experiments

Run No.	$U_{g,in}$ cm/s	Inlet Gas holdup	D_l, cm^2/s	Detector Level :	Model Parameters D_g, cm^2/s	$k_l a$ s^{-1}
R82-1	7.01	0.13	3260	1	7980	0.00676
				2	5470	0.0291
				3	7470	3.75
				4	6810	1.03
R82-2	7.01	0.13	3260	1	4130	0.00171
				2	5110	0.00214
				3	6910	0.00841
				4	7610	1.11
R86-1	12.19	0.18	3610	1	8660	1.36
				2	9850	1.12
				3	8740	0.99
				4	6590	0.75
R86-2	12.19	0.18	3610	1	7040	1.42
				2	6750	1.15
				3	8050	1.17
				4	10300	1.08

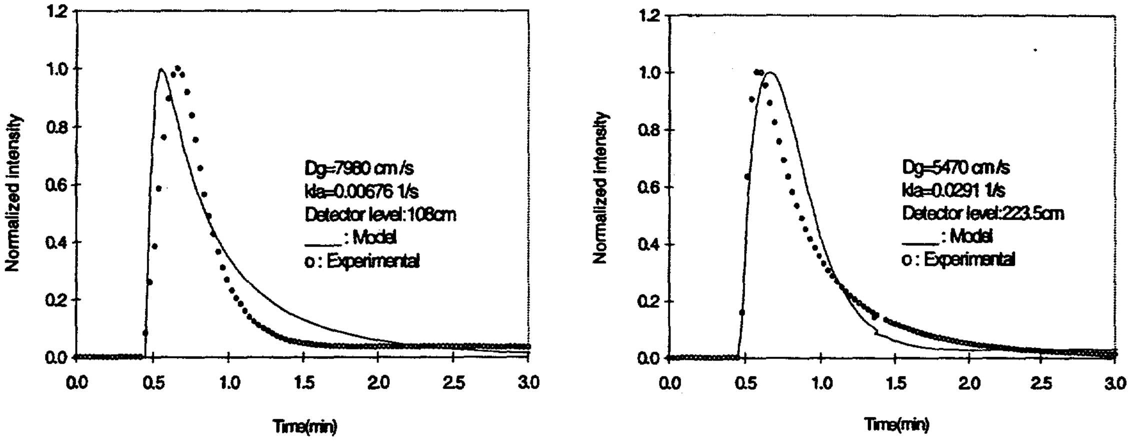

Run No. : R82-1

Run No. : R82-1

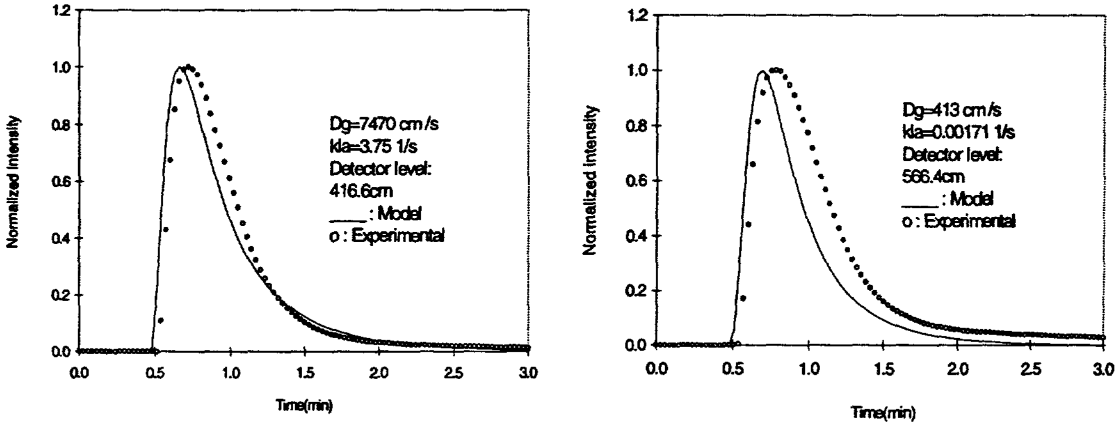

Run No. : R82-1

Run No. : R82-1

Figure 8: Case 4: Model Fits of Experimental Responses

distribution of the tracer in the entry region where the first level and second level of the detectors are mounted and the fact that at these levels the L/D is less than 3. Most likely the one dimensional model simply does not apply at these detector levels.

An investigation of the model prediction and experimental data plots shows that the model fits for Run82-1 and Run82-2 are reasonably good. However the model fits for Run86-1 and Run86-2 are somewhat off from the experimental data. It is noted that the model fits at level 4 are not as good as expected (because this level is far from the injection). As can be seen, there is a sharp increase of ε_g in the outlet region where detector level 4 is located. An underestimation of ε_g with the linear equations (Equation (1) to (4)) in the outlet region may cause bad model fits at level 4.

6.2.5 Case 5: Three Floating Parameter, D_g, $k_l a$, $l_{\min}$

As mentioned before, since the volume of gas increases due to reaction, the gas holdup and the superficial gas velocity vary in the axial direction . The outlet superficial gas velocity is almost doubled compared to that at the inlet as shown in Table 1. In an attempt to obtain better model fits, the variation of gas holdup and superficial gas velocity is taken into account in parameter estimation. The variation of gas holdup in the axial direction, which is obtained by fitting a linear function to experimental data, is given by Equations (1) to (4) for various runs. The variation of superficial gas velocity in the axial direction is also assumed to be linear in this case. However, two cases of a linear variation of U_g can be considered. One is that U_g keeps increasing from the bottom to the top of the column and reaches its maximum value at the top. The other one is that U_g increases from the bottom to some axial position between the top and the bottom and reaches its maximum value at that position $l_{\min}$, then it kept constant at the maximum value for the rest of the column. The latter case is more general because it includes the former case. The linear variation of U_g with axial coordinate z is considered as

$$U_g = U_{g,in} + \frac{U_{g,f} - U_{g,in}}{l_{\min}} z \ , \quad z \le l_{\min} \tag{19}$$

$$U_g = U_{g,f} \, , \qquad\qquad z \geq l_{\min} \qquad\qquad (20)$$

Here $U_{g,in}$ and $U_{g,f}$ are the inlet and outlet superficial gas velocity, $l_{\min}$ is the height at which U_g reaches its maximum value. This is a general case since if $l_{\min}$ is set to the slurry height, a linear variation through out the column can be obtained. A typical variation of U_g with z described by Equation (19) is shown in Figure 9.

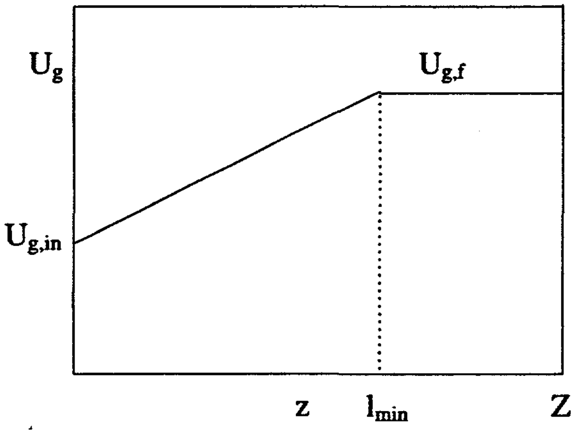

Figure 9. Illustrative Variation of U_g with Axial Position

In Equation (19), $l_{\min}$ is an unknown parameter to be estimated by fitting of the tracer response curves. Thus, model fitting of data was conducted to get D_g, $k_l a$, $l_{\min}$. Table 12 shows the results. Figure 10 displays the plots of model estimated and experimental responses. For all the runs and detector levels, the estimated $l_{\min}$ is 610 cm except for level 3 of R82-2 with the value of $l_{\min} = 555$ cm. This means that U_g increases linearly throughout the whole column. Thus, we can assume that the dehydration reaction occurs in the whole column. In this case, the axial dispersion coefficients obtained are somewhat larger than those obtained from other cases. The average D_g for $U_{g,in}$ of 7.01 cm/s and 12.19 cm/s are 8440 cm^2/s and 9860 cm^2/s, respectively, showing a large extent of back mixing of the gas phase in the column. However, the estimated mass transfer coefficient, $k_l a$, does not show any improvement regarding to the extent of variability of the estimated values. The ratio of $k_l a_{\max} / k_l a_{\min}$ remains about 950.

Table 12. Case 5: Parameter Estimation Results of Gas Tracer Experiments

Run No.	$U_{g,in}$ cm/s	Inlet Gas holdup	D_l, cm^2/s	Detector Level :	Model Parameters		
					D_g, cm^2/s	$k_l a$ s^{-1}	l_{min} cm
R82-1	7.01	0.13	3260	1	9570	0.0286	610
				2	8770	3.58	610
				3	8990	6.79	610
				4	7130	3.30	610
R82-2	7.01	0.13	3260	1	5380	0.0126	610
				2	7350	0.0202	610
				3	10800	2.85	555
				4	9470	2.47	610
R86-1	12.19	0.18	3610	1	10700	4.27	610
				2	8470	2.07	610
				3	8910	1.88	610
				4	13100	1.51	610
R86-2	12.19	0.18	3610	1	8950	12.03	610
				2	9370	2.92	610
				3	9440	2.52	610
				4	9930	1.83	610

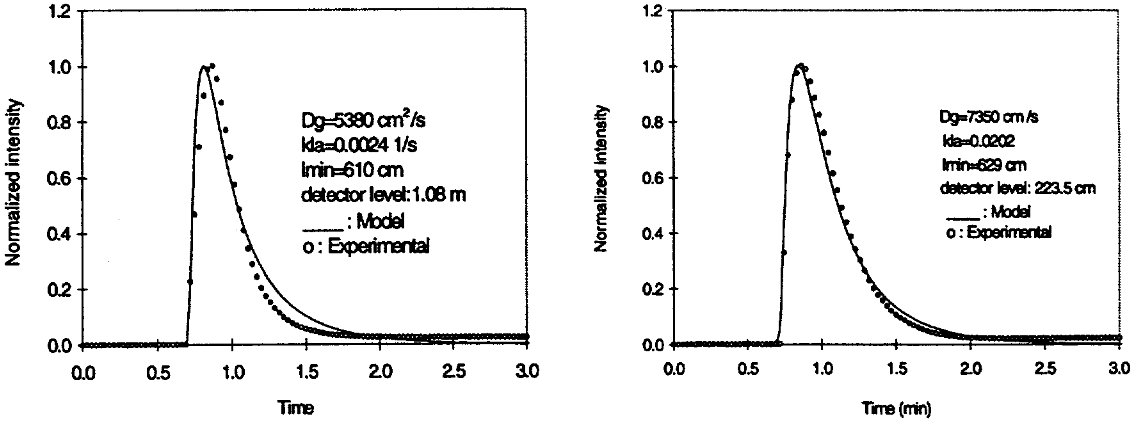

Run No. : R82-2

Run No. : R82-2

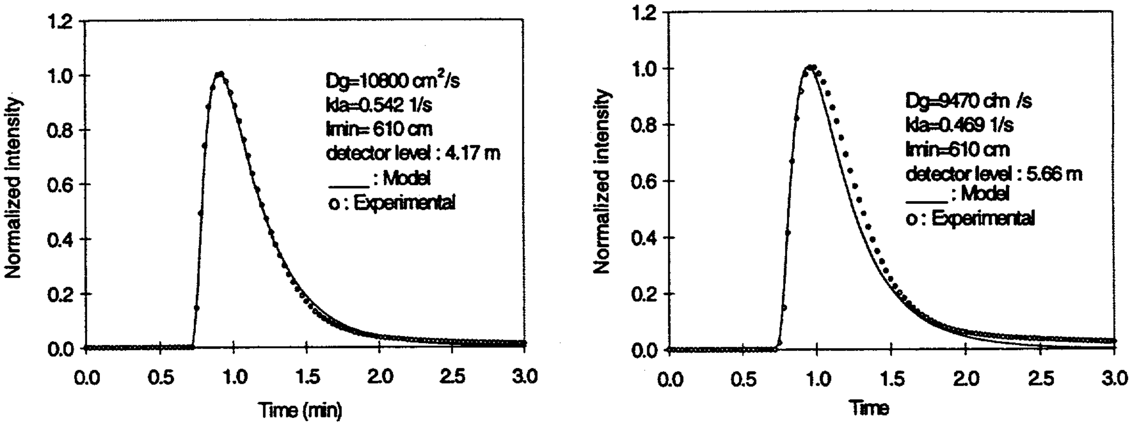

Run No. : R82-2

Run No. : R82-2

Figure 10. Case 5: Model Fits of Experimental Responses

In this case the same observation, as in Case 3 and Case 4, holds that the model fits for Run82-1 and Run82-2 are quite good, while the model fits for Run86-1 and Run86-2 are somewhat off. Also the fits at level 4 are not as good as expected due to the underestimation of the ε_g in the outlet region.

6.2.6 Case 6: Three Floating Parameters, D_g, $k_l a$, β

In this case, an exponential increase of U_g is considered. The variation of U_g with z has the form:

$$U_g = U_{g,f} + (U_{g,in} - U_{g,f})(1 - z/Z)e^{-\beta z} \tag{21}$$

Here, Z is the maximum slurry level in the reactor, 610 cm. A small β, less than 1.0×10^{-4} will give an approximate linear variation of U_g. β was estimated together with D_g and $k_l a$. However, for all runs and detector levels, the obtained value of β is almost zero, indicating a linear variation pattern of U_g. The same values of D_g and $k_l a$ are obtained as those in Case 5 for the same set of data.

6.2.7 Discussion of Results

The parameters that truly need to be estimated from this model are : the gas phase axial dispersion coefficient, D_g, and the gas-liquid phase mass transfer coefficient, $k_l a$, of which D_g is of more interest to us because it represents the extent of backmixing in the column. In order to get a clear analysis of the parameters, the mean and the standard deviations of D_g and $k_l a$ for each run are reported in Table 13 and Table 14 for all the cases considered in this study.

From Table 13, one can see that in all the cases, D_g increases with gas superficial velocity. However there is a considerable spread of D_g values around the mean, especially for Case 1 with three floating parameters. High relative standard deviations (up to 50%) are obvious in this case.

There are some empirical correlations (Mangartz and Pilhofer, 1980; Field and Davidson, 1980; Towell and Ackerman, 1972) which can be used to predict D_g, although not all the operating conditions in this study are in the range of variables considered in the correlation development. Hence, D_g is predicted only for $U_{g,in}$ = 7.01 cm/s to compare the difference between the model estimated values in this study and those predicted from correlations. The results are shown in Table 15. It is seen that the D_g predicted by correlation 1 (Towell and Ackerman, 1972) is in the same range as the values estimated from model fits of tracer data, while D_g predictions by the other two correlations are much higher than the ones obtained in this study. The same trend was observed in the model fitting of methanol synthesis system (Degaleesan et al, 1996). The reason for this is not quite clear.

Because of the high spread in values, there seems no detectable trend in k_la values with the increase in superficial gas velocity. In fact, one can see from Table 14 that, in some cases, the standard deviations are so high that they are equal to or even higher than the corresponding mean values, indicating the insensitivity of the model to the mass transfer coefficient k_la. Of the six cases, Case 2, in which the inlet gas superficial velocity $U_{g,in}$ was used as U_g for the whole column, gives the most reasonable values of k_la with the lowest range of standard deviations.

Table 16 lists the averaged gas axial dispersion coefficients and mass transfer coefficients, as well as the standard deviations for all the cases except for Case 1. It is observed that both D_g and k_la increase with the superficial gas velocity.

Table 13. Average D_g at each run for all the cases

Case No.	Run	D_g, cm^2/s	σ_D, cm^2/s
1	R82-1	2590	1140
	R82-2	3330	1970
	R86-1	6250	2990
	R86-2	3530	1990
2	R82-1	5260	1200
	R82-2	6200	898
	R86-1	6280	1930
	R86-2	6360	1480
3	R82-1	6220	595
	R82-2	8160	606
	R86-1	8370	1090
	R86-2	8890	730
4	R82-1	6930	1090
	R82-2	5940	1600
	R86-1	8460	1360
	R86-2	8050	1630
5	R82-1	8620	1050
	R82-2	8260	2390
	R86-1	10300	2110
	R86-2	9420	398
6	R82-1	8610	1050
	R82-2	8260	2390
	R86-1	10300	2110
	R86-2	9420	398

Table 14. Average $k_l a$ at each run for all the cases

Case No.	Run	$k_l a$, s^{-1}	σ_k, s^{-1}
1	R82-1	5.26	6.73
	R82-2	6.65	8.32
	R86-1	1.84	1.76
	R86-2	2.00	2.17
2	R82-1	1.62	0.60
	R82-2	1.55	0.40
	R86-1	1.02	0.18
	R86-2	1.51	0.90
3	R82-1	1.23	0.15
	R82-2	2.34	2.48
	R86-1	3.66	5.74
	R86-2	0.89	0.16
4	R82-1	1.20	1.76
	R82-2	0.27	0.55
	R86-1	1.05	0.25
	R86-2	1.20	0.15
5	R82-1	3.43	2.76
	R82-2	1.34	1.54
	R86-1	2.43	1.25
	R86-2	4.25	4.83
6	R82-1	3.43	2.76
	R82-2	1.34	1.54
	R86-1	2.43	1.25
	R86-2	4.25	4.83

Table 15. Correlations for predicting gas dispersion coefficients in bubble column

Investigators	Correlations (in SI)	Range of variables	Predicted D_g at $U_{g,in}$ =7.01 cm/s
Towell and Ackerman (1972)	$D_g = 19.7 D_c^2 U_g$	$0.00854 \le U_g \le 0.13$m/s $0.0 \le U_l \le 0.0135$cm/s D_c=0.406, 1.067 m	6630
Field and Davidson (1972)	$D_g = 56.4 D_g^{1.33} (U_g / \varepsilon_g)^{3.56}$	$0.00854 \le U_g \le 0.13$m/s $0.00724 \le U_l \le 0.0135$cm/s $0.076 \le D_c \le 3.2$ m	30300
Mangartz and Pilhofer (1980)	$D_g = 50.0 D_g^{1.50} (U_g / \varepsilon_g)^{3.00}$	$0.00854 \le U_g \le 0.13$m/s $0.00724 \le U_l \le 0.0135$cm/s D_c=0.406, 1.067 m	68300

Table 16. Averaged D_g, $k_l a$ and the corresponding deviations.

Run No.	P, psig	T, °C	$\bar{\varepsilon}_g$	$U_{g,in}$, cm/s	D_g cm^2/s	$k_l a$ s^{-1}
R82-1	25.0	300°C	0.19	7.01	6750 ±1580	1.87 ±1.77
R82-2	25.0	300°C	0.19	7.01	7140 ±1770	1.38 ±1.54
R86-1	25.0	300°C	0.25	12.19	8350 ±2010	2.04 ±2.86
R86-2	25.0	300°C	0.25	12.19	8180 ±1590	2.11 ±2.74

6.2.8 Conclusions and Future Work

Based on the model fits of tracer responses obtained in each case and the discussions above, the following conclusions are reached:

1) An investigation of the experimental data shows that the peaks for Run82-1 and Run82-2 occur at different times and long tails are observed at detectors level 1 and level 2 for Run86-1 and Run86-2. This indicates that the experiments were not repeated properly. Therefore, the variations in the estimated parameters between the two runs conducted at the same conditions are to be expected.
2) In general, good fits can be obtained with the one dimensional axial dispersion model for Run82-1 and Run82-2 which were conducted at low superficial gas velocity. However, for Run86-1 and Run86-2 only case 1, where the Henry's law constant H was treated as a floating parameter, gives reasonably good fits while different degrees of deviations between model prediction and experimental data are observed.
3) When the Henry's law constant H is treated as a floating parameter, the estimated value of H is much smaller than that calculated from thermodynamics. Meanwhile, the average estimated D_g is lower than those obtained in other cases. Fixing H at the thermodynamic value of 106 increases D_g.
4) In almost all the cases , a widely scattered range of $k_l a$ values was obtained, varying from 0.002 s^{-1} to 17.98 s^{-1}. This indicates that the model is very insensitive to the mass transfer coefficient and it is not reasonable to estimate $k_l a$ by the axial dispersion model. With low gas superficial velocities (Case 2), the mean estimated $k_l a$ has a small relative standard deviation.
5) In some cases, the estimated D_g and $k_l a$ are very low or very high for the first and second levels of the detectors. This is because the tracer needs some time, or some axial distance, to spread uniformly in the cross section after it is injected. The detectors close to the injection point cannot get good signals. In general, the fits at the lowest detector level are not as good as at the other levels.

6) The model fits at level 4 for all the cases are not as good as expected (because this level is far from the injection). This may be caused by the underestimation of ε_g with the linear variations in the outlet region.
7) In all the cases, the average value of D_g shows an increase with the increase in superficial gas velocity. However, there is a large deviation between the estimated D_g values and those predicted by empirical correlations.
8) Consideration of the axial variation of U_g and ε_g provides good fits for Run82(1 and 2). However, there is no improvement with regard to Run 86(1 and 2).
9) The average axial dispersion coefficients D_g are estimated in the range of 5000 ~ 10000 cm^2/s, indicating a considerable extent of gas backmixing in the slurry bubble column.

In summary, the axial dispersion model (ADM) is able to fit the experimental tracer data with variable accuracy. However, the drawback of it is its insensitivity to the fitting parameters, especially for $k_l a$. A model that captures better the nature of flow in bubble columns and distinguishes between the possibly different bubble sizes is required to predict the characteristics of the tracer responses at all levels in the column. For this purposes, the Two Phase Recycle with Cross-flow Model (TRCFM), which accounts for the movement of different bubble classes (gas) within the column and their interaction with the liquid phase, may be a suitable alternative.

7. Comparison with the Results from Tracer Studies in the Methanol Synthesis Slurry Bubble Column

Interpretation of the tracer data in the AFDU reactor during methanol synthesis using the ADM has already been completed (Degaleesan et al. 1996). In order to compare the results from model fitting between the present study, i.e., tracer studies during dehydration of isobutylene, and the previous study, i.e., tracer studies of methanol synthesis, we will briefly describe the operating conditions for methanol synthesis. The tracer runs were performed under high pressure (about 50 atm) and temperature (250 ^{0}C), in a column of inner diameter 18" and a dispersion height of 522". The reaction involved the synthesis of methanol from syngas, which resulted in a decrease in gas volumetric flow rate of about 20%. However experimental results for the axial gas holdup profile showed an increase in the gas holdup at higher levels in the column.

7.1 Liquid Phase Tracer

As in the case of present study, the liquid phase dispersion coefficients for the methanol synthesis runs are found to be much larger than the values predicted by literature correlations. This, in addition to effects of high pressure, can also be attributed to the non-uniform tracer injection into the column, as described earlier in this report.

The average value of D_l from the methanol synthesis runs (at U_g=14 cm/s) and those from the present study are shown in Table 17. Although the experiments during methanol synthesis were performed at higher pressure, it is seen that D_l for the present conditions are slightly higher than D_l for the methanol runs for approximately the same gas inlet velocity. This indicates that the increase in the volume of gas due to reaction, in the dehydration of isobutylene, results in larger velocities of the gas phase and, therefore, the

Table 17. Comparison of D_l Between Methanol Synthesis Runs and Present Study

System	Pressure, atm	$U_{g, in}$, cm/s	$U_{g, out}$, cm/s	D_l, cm^2/s	D_g, cm^2/s	$k_l a$, s^{-1}
Methanol synthesis	50	14.0	12.0	2713	2908	0.378
Dehydration of Isobutanol	2	7.0	13.7	3260	6946	1.62
	2	12.2	24.1	3610	8265	2.07

liquid phase, which results in a higher degree of liquid mixing. On the other hand, during methanol synthesis, there is a reduction in the volumetric flow rate of gas. In addition to this, the larger column size in the present study and the change in the configuration of the heat exchanger tubes in the column may also be factors contributing to the increase of D_l when compared with the methanol synthesis runs. All these factors compensate for the effects due to decrease in operating pressure in the present study when compared with the methanol synthesis data.

7.2 Gas Phase Tracer

Similar comparison is seen between the results for the gas phase model parameter estimation. An increase in D_g in the present calculations, from those of the methanol synthesis runs (Table 17) is attributed to the increase in gas volumetric flow rate in the column for the dehydration of isobutylene runs (present study) in contrast to the decrease in gas velocity in the methanol synthesis runs. The volumetric mass transfer coefficients for the present study are also higher than those in the methanol synthesis runs at similar gas inlet velocities (Table 17). A possible reason for this maybe the increase in gas volumetric flow rate during the dehydration of isobutylene. However, since the results from parameter estimation in the tracer studies, for both methanol synthesis and dehydration of isobutylene, show that the model is very insensitive to the mass transfer coefficient, no conclusions can be made regarding effects of process variables on the mass transfer coefficients.

8. Conclusions

The tracer data obtained in the slurry bubble column for the dehydration of isobutanol to isobutylene were interpreted with the one dimensional axial dispersion model(ADM).

For liquid phase tracer experiments, the axial dispersion model gives good fits for the responses that do not show overshoots. The mean estimated axial dispersion coefficient increases with the increase in the superficial gas velocity. However, due to the large variation in the axial dispersion coefficient obtained by fitting the data at various locations it is clear that this model cannot describe well the flow pattern and backmixing for the present system. An alternative model, the recycle Cross Flow and Dispersion Model (RCFDM) (Degaleesan, et al 1996), is proposed to describe the flow in the slurry bubble column.

For the gas tracer data analysis, the ADM fits the experimental responses well for most of the cases. Also an increase in the gas axial dispersion coefficient with superficial gas velocity is indicated. For a given run, the mass transfer coefficient, averaged for all the detector levels, increases with the increase in superficial gas velocity. However, the scatter in the mass transfer coefficient values for any particular run is large and shows no pattern with detector location. It is found that the model is not sensitive to the mass transfer coefficient, leading to a large spread in parameter values. Future work will focus on the interpretation of the gas phase tracer data with Two Phase Recycle with Cross-flow Model (TRCFM) proposed by the CREL group (Wang , 1995).

Comparison of the results between the methanol synthesis runs and the present dehydration of isobutylene studies suggests that the gas expansion in the column caused by reaction, in the present case, results in larger values for both the liquid and gas phase dispersion coefficients.

9. Nomenclature

C_g	Gas phase concentration, mol/cm^3
C_l	Liquid phase concentration, mol/cm^3
D_c	Column diameter, m
D_g	Gas axial dispersion coefficient, cm^2 /s
D_i	Fitting parameter for input pulse simulation, cm^2/s
D_l	Liquid axial dispersion coefficient, cm^2 /s

H	Henry's law constant
$K_l a$	Overall volumetric mass transfer coefficient, 1/s
$k_l a$	Liquid film volumetric mass transfer coefficient, 1/s
$k_g a$	Gas film volumetric mass transfer coefficient, 1/s
l_i	Fitting parameter for input pulse simulation, cm
$l_{\min}$	The slurry level at which U_g reaches its maximum value, cm
N_c	Fitting parameter in input pulse simulation.
t_i	Injection time, s
U_g	Superficial gas velocity, cm/s
U_{gin}	Inlet superficial gas velocity, cm/s
$U_{g,f}$	Outlet superficial gas velocity, cm/s
z	Axial position, cm
z_i	Injection position, cm
Z	The maximum slurry level, m

Greek Letters:

β	Fitting parameter
ε_g	Gas holdup
ε_l	Liquid holdup
$\delta(t)$	Liquid tracer input function (Delta function) $t \neq 0, \delta(t) = 0; \quad t = 0, \delta(t) = \infty$
$\delta(z - z_i)$	Liquid tracer input function (Delta function) $z \neq z_i, \delta(t) = 0; \quad z = z_i, \delta(t) = \infty$
$\delta_i(t)$	Gas tracer input function (Gaussian function), $\delta_i(t) = \frac{N_c}{\sqrt{2\pi D_i t}} \exp[-\frac{(l_i - U_g t)^2}{2D_i t}]$

10. Bibliography

1. Baird M. H. and Rice R. G., "Axial Dispersion in Large Unbaffled Column", Chem. Eng. J., 9,171 (1975)
2. Bhatt B. L., Liquid Phase Isobutylene Demonstration in the LaPorte Alternative Fuels Development Unit, Final Report, May, 1995
3. Decker W. D., Burchart R. and Zoll G., "Mixing and Mass Transfer in Tall Bubble Columns", Chem. Eng. Sci., 29, 2117 (1974)
4. Degaleesan S. and Dudukovic M. P. & B. L. Bhatt and B. A. Toseland, Fourth Quarterly Report for Contract. DOE-FC 2295 PC 95051(1996)
5. Degleesan S., Roy S., Kumar S. and Dudukovic M. P., "Liquid Mixing Based on Convection and Turbulent Dispersion In Bubble Column", Chem. Eng. Sci., 51(10), 1976(1996)
6. Dudukovic M. P., Tracer Methods in Chemical Reactors: Techniques and Applications, *Chemical Reactor Design and Technology* (De Lasa, H ed)NATO Series E: Applied Sciences N-110 (Nijhoff Publishing Co, Dordrecht, Holland)(1987)
7. Field R. W. and Davidson J. F., "Axial Dispersion in Bubble Column", Trans IChemE , 58:228(1980)
8. Kato Y., Nishiwaki A., Fukuda T., and Tanaka S., " The behavior of suspended solid particles and liquid in bubble column", J Chem. Eng. Japan, 112:5 (1972)
9. Mangartz K. H. and Pilhofer T., Verfahreustechnik, 40: 14 (1980)
10. Nauman E. B., Chemical Reactor Design (Wiley), 1987

11 Tarmy B. L., Chang M., Coulaloglou C. A. and Ponzi. P. R., IChemE Symp Series, No. 87:303(1982)

12. Towell G. D. and Ackerman, G. H., Proceedings of the 5 th European Symposium on Chemical Reaction Engineering, B3-1, Elsevier, Amsterdam, 1972.
13. Toseland B. A., Brown D. M., Zou B. S. and Dudukovic M. P., "Flow Pattern In a Slurry Bubble Column Reactor Under Reaction Conditions" Trans. IChemE, 73(Part A): 297(1995)
14. Tsoulfanidis N., Measurement and Detection of Radiation, McGraw Hill, New York.

15. Wang Q., A Two-Phase Cross Flow Model with Recycle and Interphase Mass Transfer for Churn Turbulent Bubble Columns, Report (June,1994-May, 1995), Chemical Reaction Engineering Laboratory, Washington University in St. Louis.